CSIRO PUBLISHING

Reproduction, Fertility and Development, 2017, **29**, 721–730
http://dx.doi.org/10.1071/RD15350

In vitro maturation affects chromosome segregation, spindle morphology and acetylation of lysine 16 on histone H4 in horse oocytes

Federica Franciosi[A,I], *Ghylene Goudet*[B,C,D,E], *Irene Tessaro*[A], *Pascal Papillier*[B,C,D,E], *Rozenn Dalbies-Tran*[B,C,D,E], *Fabrice Reigner*[F], *Stefan Deleuze*[G], *Cecile Douet*[B,C,D,E], *Ileana Miclea*[H], *Valentina Lodde*[A] *and Alberto M. Luciano*[A]

[A]Reproductive and Developmental Biology Laboratory, Department of Health, Animal Science and Food Safety, University of Milan, via Celoria, 10, Milan, 20133, Italy.
[B]INRA, UMR85 Physiologie de la Reproduction et des Comportements, Nouzilly, F-37380, France.
[C]CNRS, UMR7247, Nouzilly, F-37380, France.
[D]Université François Rabelais, 60 Rue du Plat d'Étain, Tours, F-37000, France.
[E]IFCE, Nouzilly, F-37380, France.
[F]INRA, UEPAO, Nouzilly, F-37380, France.
[G]Université de Liège, Clinique des Animaux de Compagnie et des Équidés, Place du 20 Août 7, Liège, 4000, Belgium.
[H]University of Agricultural Sciences and Veterinary Medicine, Calea Mănătur 3-5, Cluj-Napoca 400372, Romania.
[I]Corresponding author. Email: federica.franciosi1@unimi.it

Abstract. Implantation failure and genetic developmental disabilities in mammals are caused by errors in chromosome segregation originating mainly in the oocyte during meiosis I. Some conditions, like maternal ageing or *in vitro* maturation (IVM), increase the incidence of oocyte aneuploidy. Here oocytes from adult mares were used to investigate oocyte maturation in a monovulatory species. Experiments were conducted to compare: (1) the incidence of aneuploidy, (2) the morphology of the spindle, (3) the acetylation of lysine 16 on histone H4 (H4K16) and (4) the relative amount of *histone acetyltransferase 1* (*HAT1*), *K*(*lysine*) *acetyltransferase 8* (*KAT8*, also known as *MYST1)*, *histone deacetylase 1* (*HDAC1*) and *NAD-dependent protein deacetylase sirtuin 1 (SIRT1*) mRNA in metaphase II stage oocytes that were *in vitro* matured or collected from peri-ovulatory follicles. The frequency of aneuploidy and anomalies in spindle morphology was increased following IVM, along with a decrease in H4K16 acetylation that was in agreement with our previous observations. However, differences in the amount of the transcripts investigated were not detected. These results suggest that the degradation of transcripts encoding for histone deacetylases and acetyltransferases is not involved in the changes of H4K16 acetylation observed following IVM, while translational or post-translational mechanisms might have a role. Our study also suggests that epigenetic instabilities introduced by IVM may affect the oocyte and embryo genetic stability.

Additional keywords: aneuploidy, histone acetyl-transferases, histone deacetylases, meiosis.

Received 28 August 2015, accepted 12 November 2015, published online 14 December 2015

Introduction

Implantation failure, miscarriages and genetic developmental disabilities in mammals are often caused by errors in chromosome segregation that result in aneuploidy. Most of these errors originate in the oocyte during meiosis I (Hassold and Hunt 2001). Despite efforts to unravel the underlying molecular basis of chromosomal mis-segregation, a defined mechanism has not been identified. Several genetic, epigenetic and biochemical mechanisms have been proposed from different research groups, including defective spindle assembly checkpoint (Jones and Lane 2013; Yun *et al.* 2014), weakened centromere cohesion (Chiang *et al.* 2010; Eichenlaub-Ritter 2012; Tsutsumi *et al.* 2014), alterations in the pattern of histone covalent modifications (Akiyama *et al.* 2006; Yang *et al.* 2012; Luo *et al.* 2013;

Ma and Schultz 2013), altered microtubule–kinetochore interactions (Shomper *et al.* 2014), sites and level of recombination (Cheng *et al.* 2009; Shin *et al.* 2010; Li *et al.* 2011), cell cycle regulation defects (Homer *et al.* 2005; Nabti *et al.* 2014) and mitochondrial dysfunction (Bartmann *et al.* 2004; Eichenlaub-Ritter *et al.* 2004). While this intricate scenario likely indicates that the origin of aneuploidy is multifactorial and aneuploidies arise from different mechanisms, some conditions in the mother, such as age (te Velde and Pearson 2002) or obesity (Luzzo *et al.* 2012), are known to increase the occurrence of chromosomal mis-segregation. Moreover, a higher incidence of aneuploidy has also been described following *in vitro* maturation (IVM; Nogueira *et al.* 2000; Emery *et al.* 2005; Roberts *et al.* 2005; Nichols *et al.* 2010), indicating that events that take place in a short time period (hours) can be sufficient to induce errors in chromosome segregation.

Using an adult, naturally cycling, monovulatory animal model (the horse), we recently observed that in oocytes that were *in vitro* matured the global acetylation pattern of histone H4 at the residue lysine (K) 16 was altered following IVM compared with *in vivo*-matured oocytes. Remarkably, other H4 N-terminal K residues such as K8 and K12 were not affected (Franciosi *et al.* 2012). In the present study we investigated whether, in the same animal model, IVM can also affect the ability to form a regular spindle and normal chromosome segregation. Global acetylation at H4K16 is thought to be one of the key epigenetic regulators in somatic and germ cells, especially for chromatin remodelling and chromosome condensation (Ma and Schultz 2013). Therefore, even though its function during meiosis is not clear, it is likely that the alteration of H4K16 acetylation affects chromosomal alignment during meiosis I.

In somatic cells histone acetylation is generally associated with active gene transcription (as reviewed in Clayton *et al.* 2006; Turner 2014; Zentner and Henikoff 2014). However, a transcriptionally inactive state is established during the last phase of oocyte growth and maturation. The regulation of gene expression at this time, and until the embryonic genome is activated, relies on post-transcriptional events of previously stored maternal mRNAs (Chen *et al.* 2011). One of the described post-transcriptional regulatory mechanisms consists in the selective degradation of specific maternal mRNAs (Chen *et al.* 2011; Ma *et al.* 2013).

The interplay between several classes of histone deacetylases (HDACs) and histone acetyltransferases (HATs) is responsible for acetylation at specific histone residues (Lombardi *et al.* 2011; Marmorstein and Zhou 2014). Therefore, in the present study we investigated the total mRNA amount of four histone acetylation-related enzymes – *HAT1*, *K*(*lysine*) *acetyltransferase 8* (*KAT8*, also known as *MYST1*), *HDAC1* and *NAD-dependent protein deacetylase sirtuin 1* (*SIRT1*) – in horse oocytes that were matured *in vivo* or *in vitro*. With this study we started to investigate the molecular mechanism that might interfere with the acetylation state of H4K16 during IVM.

Compared with rodent animal models, the horse does not allow genetic manipulations, is less easy to manipulate and its maintenance is more expensive. However, because of the similarity in the ovarian follicular waves and ovulation of one dominant follicle to human ovarian physiology, the horse model is gaining considerable interest for the study of oocyte maturation (Ginther *et al.* 2004; Carnevale 2008; Donadeu and Pedersen 2008; Ginther 2012), oocyte quality (Cox *et al.* 2015) and as a model of reproductive aging (Campos-Chillon *et al.* 2015; Hendriks *et al.* 2015; Ruggeri *et al.* 2015).

Materials and methods

All the procedures were approved by the Animal Care and Use Committee CEEA Val de Loire Number 19 and performed in accordance with the Guiding Principles for the Care and Use of Laboratory Animals.

All chemicals were purchased from Sigma-Aldrich (St. Quentin Fallavier, France or Milan, Italy) unless otherwise indicated.

Oocyte collection and in vitro *maturation*

Oocytes were collected by transvaginal ultrasound-guided aspiration from 32 adult cyclic pony mares (3–12 years old) housed at the facilities of INRA, Nouzilly. Based on mare reproductive physiology, standard breeding and veterinary practice and previous studies (Carnevale 2008; Rambags *et al.* 2014; Campos-Chillon *et al.* 2015; Ruggeri *et al.* 2015) mares 3–12 years old were used because they are considered to be young but already mature in terms of reproductive performance. Collection procedures were conducted as previously described (Luciano *et al.* 2006; Franciosi *et al.* 2012). Briefly, the ovaries were daily assessed by ultrasound scanning and at the emergence of a follicle ≥33 mm the mares were injected i.v. with 1500 IU human chorionic gonadotrophin (hCG; Chorulon; Intervet, Beaucouzé, France). The *in vivo*-matured oocytes (one per mare) were collected by transvaginal ultrasound-guided aspiration of the pre-ovulatory follicle 35 h after hCG injection. Only oocytes with a well-extruded polar body (28/32: 88% maturation rate) were considered to be mature and further used in downstream procedures (16 for immunofluorescence and 12 for reverse transcription quantitative polymerase chain reaction (RT-qPCR), respectively); the others were discarded.

Fifty-eight germinal vesicle (GV)-stage oocytes were collected from follicles ≥5 and ≤25 mm in diameter. Attempts to retrieve GV-stage oocytes from follicles ≥33 mm of mares not treated with hCG were not successful because of the limited number of follicles at this stage of development. Fourteen of those collected were used for mRNA extraction, while the remaining 44 were matured *in vitro* as previously described (Franciosi *et al.* 2012) and used in downstream procedures (25 for immunofluorescence and 12 for RT-qPCR, respectively). Briefly, IVM procedures consisted of culture in TCM199 supplemented with 20% fetal calf serum (FCS; Gibco by Life Technologies, Carlsbad, CA, USA), 0.68 mM L-glutamine, 25 mM NaHCO3, 0.2 mM sodium pyruvate and 50 ng mL^{-1} epidermal growth factor in humidified air with 5% CO_2 at 38.5°C for 28 h. Only oocytes that after 28 h IVM showed a well-extruded polar body (37/44: 85% maturation rate) were considered to be mature and further used in downstream procedures; the others were discarded.

Chromosome count

Chromosome-counting procedures were adapted from Duncan *et al.* (2009) and Chiang *et al.* (2010). After 28 h IVM or after collection from the pre-ovulatory follicle, the cumulus-enclosed oocytes were cultured for 1 h in the presence of 100 μM monastrol. The cumulus cells were then removed by treatment in 0.5% hyaluronidase or by gentle pipetting and the zona pellucida was digested in 0.2% pronase. The oocytes were fixed in 4% paraformaldehyde in phosphate-buffered saline (PBS) for 15 min at 38.5°C followed by a further 45 min at 4°C, extensively washed in PBS–polyvinyl alcohol (PVA) and permeabilised in 0.3% Triton X-100 for 10 min at room temperature. Non-specific binding was blocked by incubation in PBS with 1% bovine serum albumin (BSA) and 10% normal donkey serum for 30 min at room temperature. Oocytes were then incubated in a solution of rabbit anti-Aurora B phospho-Thr232 (636102; Biolegend, San Diego, CA, USA) in PBS with 1% BSA (dilution 1 : 50) at 4°C overnight. After extensive washing, the oocytes were incubated in a solution of tetramethylrhodamine isothiocyanate (TRITC)-conjugated donkey anti-rabbit IgG (1 : 100 in PBS with 1% BSA) for 1 h at room temperature in the dark, then washed again and mounted on slides in the anti-fade medium VectaShield (Vector Laboratories Inc., Burlingame, CA, USA) supplemented with 20 μM YOPRO1 (Invitrogen by Life Technologies).

The samples were analysed on a laser-scanning confocal microscope (LSM 780; Zeiss, Oberkochen, Germany). Images were taken spanning the whole metaphasic plate on the z-axis every 0.35 μm. The chromosome number was counted in serial confocal sections by using NIH ImageJ 1.4 Software (rsb.info.nih.gov/ij/download.html). Specifically, the serial sections are piled, but only one layer is visualised at a time. By going back and forth from one section to the other, chromosomes that appear, stay and disappear in sequential sections are identified with a numeric code. The centromere marker, by staining a much smaller volume compared with the chromosome volume, allows tracking of the overlapping chromosomes that are otherwise hardly distinguishable on the 2D reconstructed image.

The staining of the centromeric region with the Aurora B phospho-(Thr232) was used to identify different chromosomes on sequential plans. The chromosomal count was carried out blindly by two independent operators and expressed as 32 (euploid), >32 (hyperploid) or <32 (hypoploid).

Spindle and acH4K16 immunostaining

Immunostaining procedures were adapted from Goudet *et al.* (1997). Cumulus cells were removed by treatment in 0.5% hyaluronidase or by gentle pipetting, briefly washed in Dulbecco's PBS with 0.1% PVA and fixed in 2.5% paraformaldehyde for 20 min at 38°C. The oocytes were then washed, permeabilised in 0.1% Triton X-100 for 5 min at room temperature and non-specific binding was blocked by incubation with 10% normal donkey serum, 2% BSA and 0.05% saponin for 2 h at room temperature. The oocytes were incubated overnight at 4°C in a solution of mouse anti-α-tubulin (1 : 150) and rabbit anti-acH4K16 (1 : 250; Upstate Biotechnology Inc., Lake Placid, NY, USA) in PBS with 2% BSA and 0.05% saponin. After extensive washing, the oocytes were incubated in a solution of AlexaFluor 488-coniugated donkey anti-mouse IgG (1 : 500; Invitrogen by Life Technologies) and TRITC-conjugated donkey anti-rabbit IgG (1 : 100; Vector Laboratories Inc.) in PBS with 2% BSA and 0.05% saponin for 1 h at room temperature in the dark. After extensive washing, the samples were mounted on slides in VectaShield supplemented with 1 μg mL^{-1} 4′,6-diamidino-2-phenylindole (DAPI).

Samples were analysed using a confocal laser-scanning microscope (LSM 700; Zeiss) with a 60× objective. Digital optical sections were obtained by scanning the samples on the z-axis at 0.29 μm thickness throughout the whole spindle. The z-series were then projected to obtain a three-dimensional image. Instrument settings for the red and blue channels (acH4K16 and DNA, respectively) were kept constant.

Image analysis was carried out using NIH ImageJ 1.4 Software. The spindle diameter and length were measured three times for each sample and the mean of the three measurements was considered for further analysis. The quantification of the relative fluorescence of acH4K16 was measured on digitised images and normalised to DAPI staining, representing total DNA.

RNA purification, reverse transcription and polymerase chain reaction

After cumulus cells removal, the oocytes were washed in PBS–PVA and collected singly in 1 μL at the bottom of a microtube. The granulosa cells from two to five 5–25-mm follicles were pooled and washed twice in cold PBS by centrifuging at 10 600*g* for 2 min at room temperature. The samples were covered with 2 μL RNA Later (Ambion, Huntingdon, UK) and snap frozen at the end of each collection session. For the RNA extraction the oocytes were pooled two by two in the extraction buffer of the PicoPure RNA Isolation Kit (Arcturus by Life Technologies, Saint Aubin, France) and 2 pg of *Luciferase* RNA (Promega, Charbonnières-les-bains, France) were added as an external standard. Six or seven pools of oocytes for each experimental group (GV, *in vivo* matured and *in vitro* matured) were processed. Total DNase-treated RNA was extracted from oocytes and granulosa cells following the manufacturer's instructions.

The RNA was reverse transcribed in 10 μL with 0.25 μg random hexamers and mouse Moloney leukaemia virus reverse transcriptase (Invitrogen) for 1 h at 37°C. Real-time PCR was performed on a MyiQ Cycler apparatus (Bio-Rad, Marnes-la-Coquette, France). Reactions were performed in a total volume of 20 μL using cDNA equivalent to 0.05 oocytes as substrate, SYBR green Bio-Rad supermix and 0.3 μM of each specific primer (Table 1). A three-step protocol (95°C for 30 s, 60°C for 30 s, 72°C for 20 s) was repeated for 40 cycles, followed by acquisition of the melting curve. Serial dilutions of a known amount of cDNA, ranging from 50 to 0.01 ng, derived from the follicular granulosa cells, were used to calculate a standard curve and assess the starting quantity (SQ) of the specific mRNA in the oocyte samples, considering the median value of triplicate reactions. The expected amplicon sizes are shown in Table 1. The data are expressed as the ratio between the SQ of the gene of interest and the SQ of *GAPDH*, representing the housekeeping gene.

Table 1. List of primers

Target gene	Forward primer	Reverse primer	Amplicon size
GAPDH	ATCACCATCTTCCAGGAGCGAGA	GTCTTCTGGGTGGCAGTGATGG	241 bp
HAT1	CTGACATGAGTGATGCTGAACA	TAACGCGTCGGTAATCTTCC	219 bp
HDAC1	GAAGGCGGTCGCAAGAAT	CCAACTTGACCTCCTCCTTGA	166 bp
KAT8	ACTGGTCTTGGGTCCTGCTG	GGGCACTTTTGAGGTGTTCC	198 bp
Luciferase	TCATTCTTCGCCAAAAGCACTCTG	AGCCCATATCCTTGTCGTATCCC	148 bp
SIRT1	GACTCGCAAAGGAGCAGATT	GGACTCTGGCATGTTCCACT	169 bp

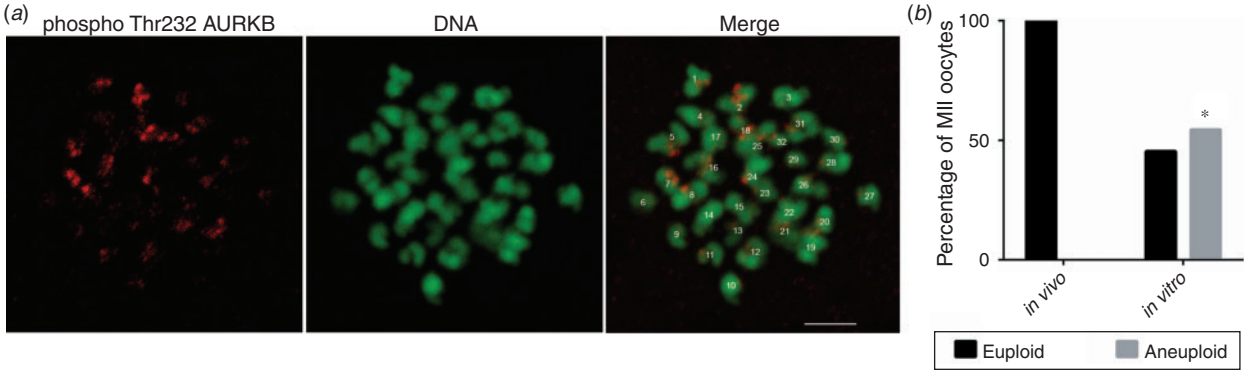

Fig. 1. Chromosome count in *in vivo*- and *in vitro*-matured oocytes. (*a*) Representative images showing aurora B phospho-Thr232 (red) and DNA (green) staining of a MII-stage horse oocyte treated with monastrol. The merge between the red and green staining has been used to count the chromosomes. An euploid oocyte (32 chromosomes) is shown. Scale bar = 5 μm. (*b*) The bar graph represents the distribution of euploid and aneuploid MII-stage oocytes in *in vivo*- ($n = 12$) and *in vitro*- ($n = 11$) matured oocytes. *Indicates significant difference in the aneuploidy rate (Fisher's exact test, $P < 0.05$).

Statistical analysis

The aneuploidy rate between *in vitro*- and *in vivo*-matured oocytes was compared by Fisher's exact test. Data on the spindle diameter, spindle length and the relative fluorescence of acH4K16 were analysed by unpaired *t*-test. The Pearson coefficient (*r*) was calculated to express the correlation between acH4K16 and spindle length, and between acH4K16 and spindle diameter. Real-time PCR data were analysed by one-way ANOVA. *P* values <0.05 were considered to be statistically significant. Results are presented as mean ± s.e.m. unless otherwise specified.

Results

The incidence of aneuploidy is increased in in vitro*-matured oocytes*

In order to study whether IVM can perturb the chromosome–spindle interaction during the first meiotic division, the number of chromosomes at the MII stage was counted, as it represents the result of chromosome segregation during meiosis I. Antibodies anti-CENPA (ab13939; Abcam, Cambridge, UK) and anti-AURKB (ab3609; Abcam) failed to localise to the centromeres in MII-stage horse oocytes (data not shown). In our hands, the anti-Aurora B phospho-Thr232 antibody was considered a good marker for the centromeric region in horse oocytes (Fig. 1*a*).

In vitro-matured oocytes had a significantly higher percentage of aneuploidy (5/11) when compared with *in vivo*-matured oocytes (0/12; Fisher's exact test, $P < 0.05$; Fig. 1*b*). Specifically, 4/5 of the aneuploid *in vitro*-matured oocytes were hyperploid, with a chromosomal count >32, while one oocyte was hypoploid, with a chromosomal count of 28. Examples of euploid and aneuploid chromosomal counts carried out on sequential confocal sessions are given in Fig. S1, available as Supplementary Material to this paper.

Spindle anomalies are increased in in vitro*-matured oocytes and correlate with H4K16 deacetylation*

Representative images of bipolar (normal) and irregular spindles are given in Fig. 2 (also see Supplemental Movie for an example of a monopolar spindle). Fifty per cent of the *in vitro*-matured oocytes showed evident morphological anomalies, like multipolar or monopolar spindles (4/14) and chromosomes scattered throughout the spindle structure (3/14), whereas all the *in vivo*-matured oocytes (4/4) showed bipolar spindles with chromosomes aligned on the metaphasic plate. The structure of the spindle looked more compact in *in vivo*-matured oocytes when compared with the *in vitro*-matured ones, which is in agreement with a previous report in mice (Sanfins *et al.* 2003).

In order to confirm this morphological observation, the diameter of the spindle was measured at the maximum width at the metaphasic plate level; the spindle length was considered

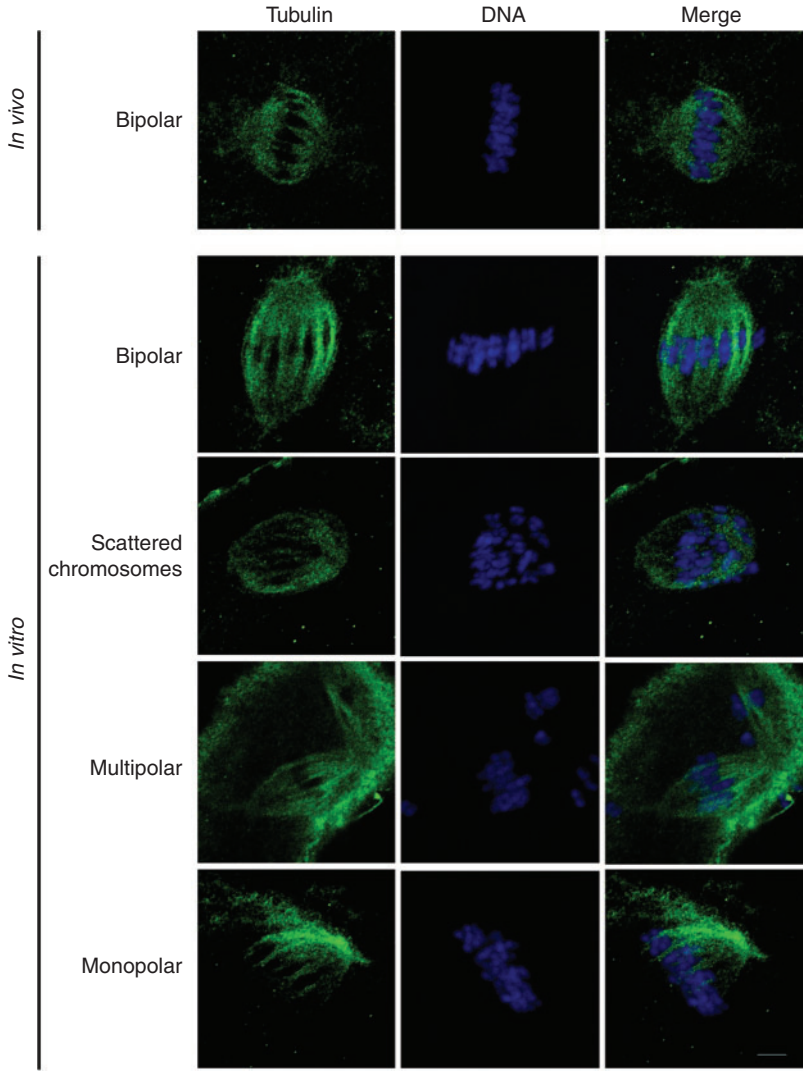

Fig. 2. Spindle morphology in *in vivo*- and *in vitro*-matured oocytes. Representative images showing tubulin (green) and DNA (blue) staining in MII-stage horse oocytes after *in vivo* ($n = 4$) or *in vitro* ($n = 14$) maturation. Examples of bipolar, multipolar and monopolar spindles and of chromosomes scattered throughout the spindle are given. Scale bar = 5 μm.

to be the maximal distance between the two poles (Fig. 3*a*). These measurements demonstrated that *in vitro*-matured oocytes have a significantly larger diameter (17.28 ± 0.81 μm) and pole-to-pole distance (19.89 ± 1.15 μm) compared with *in vivo*-matured oocytes (13.56 ± 0.91 μm diameter and 14.57 ± 1.7 μm length; unpaired *t*-test, $P < 0.05$). Even though not statistically significant ($P = 0.1286$), the acetylation level of H4K16 was negatively correlated with the length of the spindle ($r = -0.42$; Fig. 3*b*). No correlation was observed between H4K16 acetylation and spindle diameter ($r = -0.12$; Fig. 3*c*, $P = 0.5902$).

Overall, the global acetylation at H4K16 was significantly lower in IVM oocytes compared with their *in vivo* counterparts (Fig. 3*a* and Fig. S2), confirming our previous results.

Expression of transcripts encoding for histone acetyltransferases (HATs) and deacetylases (HDACs) during horse oocyte maturation

We investigated whether differences in histone H4 acetylation between *in vitro*- and *in vivo*-matured oocytes were associated with altered expression of four genes involved in this process: two HATs (*HAT1* and *KAT8*) and two HDACs (*HDAC1* and *SIRT1*). Relative mRNA expression was assessed by real-time PCR in seven pools of GV-stage, seven pools of *in vivo*-matured and six pools of *in vitro*-matured oocytes (Fig. 4). We did not observe any significant difference in the expression of *HAT1*, *KAT8*, *HDAC1* or *SIRT1* between the three classes of oocytes, independent of the meiotic stage or the maturation conditions.

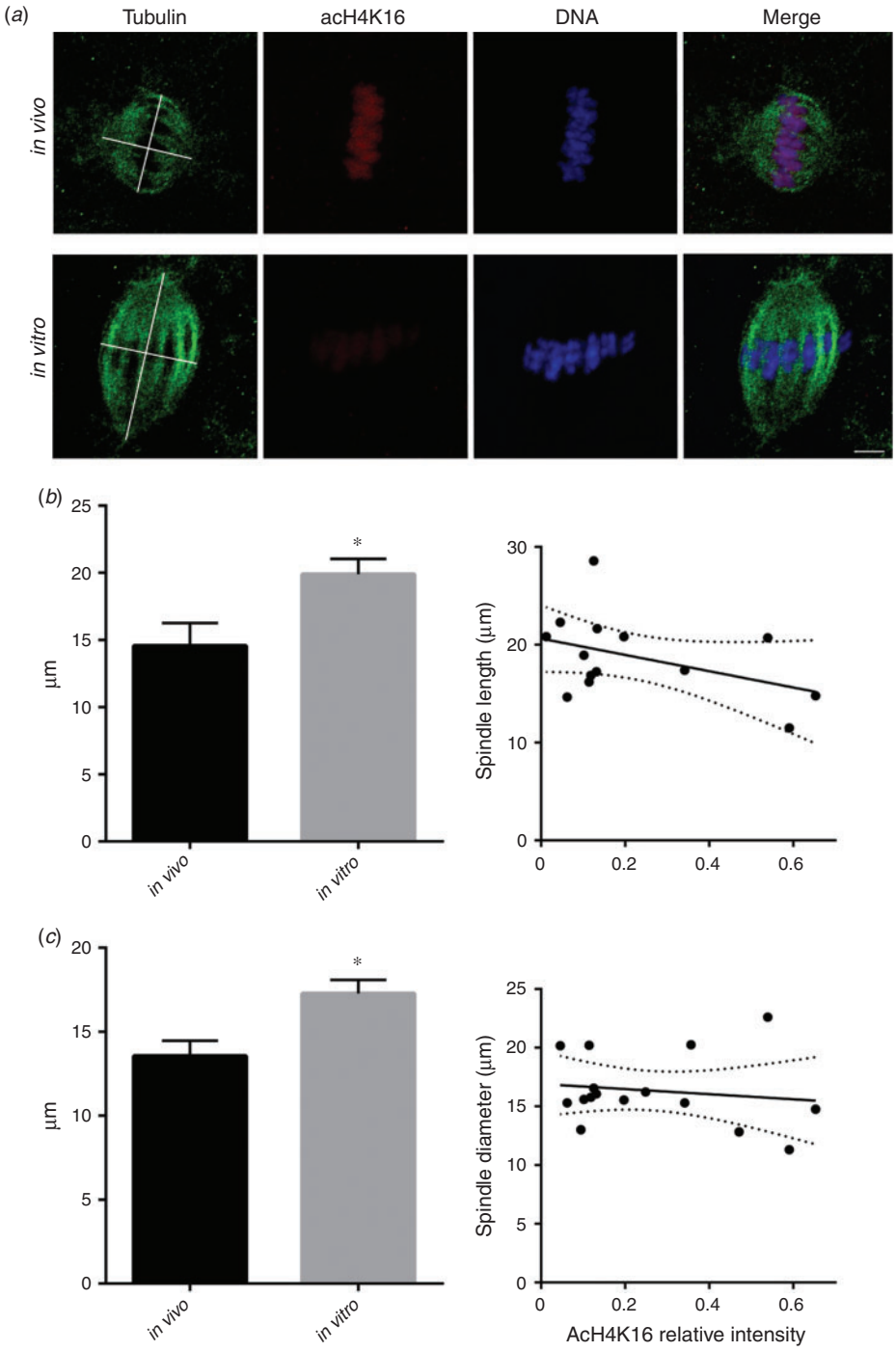

Fig. 3. Measurement of spindle length and diameter and correlation with H4K16 acetylation. (*a*) Representative images showing tubulin (green), acetylated H4K16 (red) and DNA (blue) in MII oocytes after *in vivo* ($n = 4$) or *in vitro* maturation ($n = 14$). The tubulin images show the axes used for spindle length and diameter measurements. Scale bar = 5 μm. (*b*) The bar graph represents the measurement (mean ± s.e.m.) of the spindle length in MII-stage oocytes after *in vivo* ($n = 4$) or *in vitro* ($n = 14$) maturation. The line graph represents the correlation between spindle length and acetylation at H4K16 ($r = -0.42$). (*c*) The bar graph represents the measurement (mean ± s.e.m.) of the spindle diameter in MII-stage oocytes after *in vivo* ($n = 4$) or *in vitro* ($n = 14$) maturation. The line graph represents the correlation between spindle diameter and acetylation at H4K16 ($r = -0.12$). *Indicates significant difference between *in vivo* and *in vitro* maturation (unpaired *t*-test, $P < 0.05$).

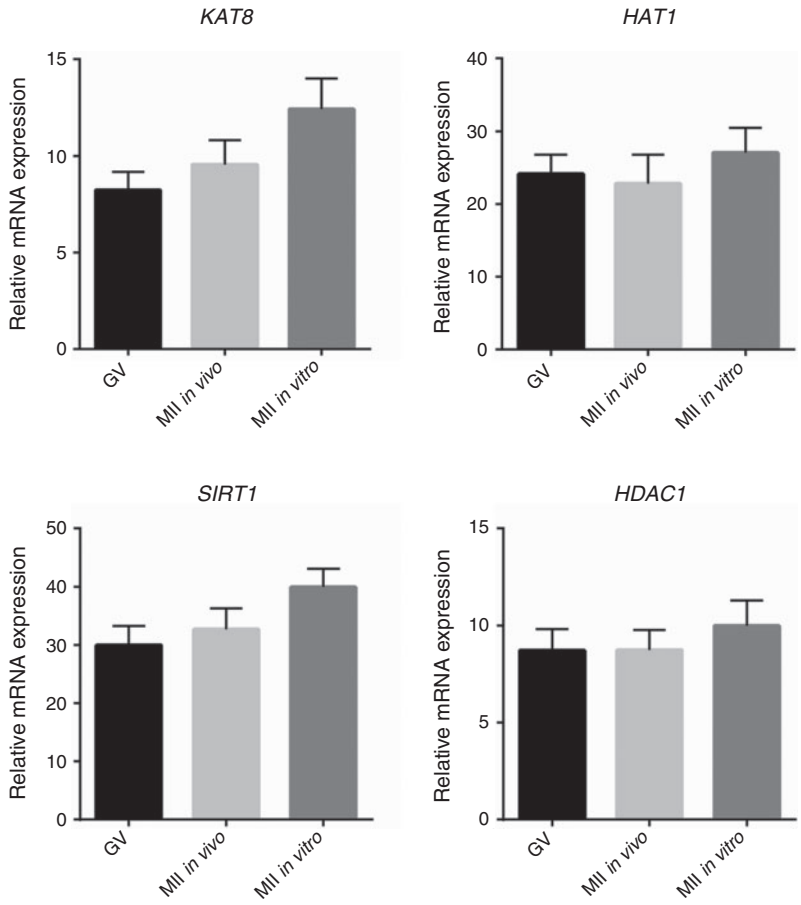

Fig. 4. Expression of *KAT8*, *SIRT1*, *HAT1* and *HDAC1* in GV-stage, *in vivo*- and *in vitro*-matured oocytes. The bar graphs represent the relative mRNA expression of *KAT8*, *SIRT1*, *HAT1* and *HDAC1* expressed as the starting quantity (SQ) of the gene of interest compared with the SQ of *GAPDH*, used as a housekeeping gene. No statistical differences were observed between GV ($n = 14$), *in vivo*- ($n = 14$) and *in vitro*- ($n = 12$) matured oocytes (one-way ANOVA, $P > 0.05$).

Similar results were obtained by normalising the mRNA relative abundance against the spike-in mRNA *Luciferase* (Fig. S3).

Discussion

Oocyte *in vitro* maturation (IVM) represents a less drug-oriented, less expensive and more patient-friendly approach in assisted reproductive technology (ART) compared with ovarian hormonal stimulation. However, the use of IVM in human infertility treatment is still limited because it can increase the incidence of aneuploidy (Nogueira *et al.* 2000; Emery *et al.* 2005; Requena *et al.* 2009) with consequent risk of embryo–fetal loss and genetic diseases. A deeper knowledge of the molecular basis of chromosomal mis-segregation during IVM will increase the possibilities of developing safer IVM procedures. Here we propose the use of a monovulatory animal model, the mare, to investigate the process of oocyte maturation and to compare *in vivo* and *in vitro* conditions.

We first tested whether the occurrence of errors in chromosome segregation was increased in *in vitro*-matured horse oocytes, as happens in humans (Nogueira *et al.* 2000; Emery *et al.* 2005). A previous study, where the ploidy of horse embryos was investigated by fluorescent *in situ* hybridization (FISH), indicates that the nuclei of *in vitro*-produced embryos are more likely to be affected by chromosomal abnormalities than *in vivo*-produced embryos (Rambags *et al.* 2005). However, despite the fact that IVM has been performed in horses for more than 20 years (Choi *et al.* 1993; Hinrichs *et al.* 1993), whether the oocyte can be the origin of embryonic aneuploidy has never been tested. The reason can partially reside in the fact that the preparation of oocyte spreads for chromosome counting usually results in considerable sample loss. With this in mind, we adapted a technique recently described in mouse oocytes (Duncan *et al.* 2009; Chiang *et al.* 2010) where the kinesin-5 inhibitor monastrol was used to collapse the spindle and disperse the chromosomes. This treatment allowed us to count the chromosomes without preparation of chromosomal spreads.

We observed that *in vitro*-matured oocytes are significantly more prone to undergo defects in chromosome segregation during meiosis I compared with their *in vivo* counterparts. These results demonstrate that aneuploidies in horses can originate in the oocyte during meiosis I, similar to what has been described in humans (Hassold and Hunt 2001). Notably, the incidence of aneuploidy that we observed in IVM oocytes was higher than the one reported for *in vitro*-produced embryos (Rambags *et al.* 2005), possibly suggesting that severe aneuploidies are not compatible with early embryonic development. Overall our results indicate that horse oocytes could be a valid cellular model for studying human aneuploidy during IVM compared with mouse oocytes, which are only minimally affected by aneuploidy.

In a second set of experiments we analysed the morphology of the meiotic spindle in *in vivo*- and *in vitro*-matured oocytes. Some spindle anomalies, such as monopolar or multipolar spindles or chromosomes scattered throughout the spindle rather than aligned at the spindle equator, were observed in *in vitro*-matured oocytes, in agreement with previous studies (Goudet *et al.* 1997). *In vivo*-matured oocytes instead consistently showed a compact structure and bipolar morphology. Further morphometric analysis also demonstrated that bipolar, apparently normal, IVM spindles are significantly longer and wider compared with *in vivo* ones. Our observations on horse oocytes support the hypothesis that aneuploidies can arise from defective spindle formation during IVM, as already proposed by Sanfins *et al.* (2003), i.e. that altering the proper tension of microtubules can interfere with normal chromosome segregation.

In a recent study we observed that IVM also affects the acetylation pattern of H4K16, while residues K8 and K12 were not altered (Franciosi *et al.* 2012). Specifically H4K16 is acetylated at the GV stage. Upon maturation H4K16 remains acetylated in *in vivo*-matured oocytes, while it undergoes deacetylation following IVM.

In somatic cells, H4K16 deacetylation is generally thought to be necessary for chromatin condensation and silencing of gene expression (Shogren-Knaak *et al.* 2006). However, other studies have demonstrated that acetylated H4K16 can be found in association with repressor proteins (Robin *et al.* 2007) and whether acetylated H4K16 inhibits or promotes the chromatin-remodelling complex ATPase Imitation of SWI (ISWI), is still a matter of debate (Klinker *et al.* 2014).

In the case of the transcriptionally inactive MII-stage oocytes, the global H4K16 acetylation can hardly be related to active gene expression, while a role in chromatin condensation seems more likely. We hypothesise that acetylated H4K16 promotes the recruitment of factors necessary for proper chromosome aggregation and for the interactions with proteins of the meiotic apparatus. This hypothesis is partially supported by the observation that one of the spindle anomalies found in IVM horse oocytes correlates with the deacetylation of H4K16, but this still requires extensive testing.

Studies conducted in a mouse model null for *histone deacetylase 2* (*Hdac2*$^{-/-}$) showed that the hyperacetylation of H4K16 is associated with weakened kinetochore–microtubule attachment and increased chromosome segregation errors (Ma and Schultz 2013). These results are only apparently in conflict with our hypothesis. In fact, they demonstrate that perturbing the acetylation pattern of H4K16 leads to aneuploidies and alters chromosome–spindle interactions. Importantly, both studies agree that a normal acetylation state (*in vivo*-matured horse oocytes and wild-type mice) is associated with proper chromosome segregation and normal spindle assembly.

During oocyte maturation chromatin is transcriptionally inactive and the control of gene expression is exerted at the cytoplasmic level through the regulation of translation, storage and degradation of specific transcripts (Chen *et al.* 2011; Ma *et al.* 2013). In this view we reasoned that IVM could interfere with such regulatory mechanisms, for instance by promoting the degradation of mRNAs involved in histone acetylation or by inhibiting the degradation of deacetylase transcripts. To test this hypothesis we investigated the relative mRNA abundance of four transcripts, two encoding for HATs and two encoding for HDACs. For each class we analysed one enzyme known to have a broad activity on different H4 K-residues (*HAT1* and *HDAC1*, for the acetyltransferases and deacetylases, respectively; Parthun 2007; Ma and Schultz 2008) and one more specific to K16 (*KAT8-MYST1* and *SIRT1* for the acetyltransferases and deacetylases, respectively; Peng *et al.* 2012; Marmorstein and Zhou 2014). We did not observe significant differences between *in vivo* and *in vitro* maturation in the expression of any of the genes considered. Our results demonstrate that impaired stability or degradation of *HAT1*, *KAT8*, *HDAC1* and *SIRT1* transcripts is not the mechanism responsible for the alteration of the pattern of histone acetylation during IVM. Even though we cannot exclude the involvement of other HATs or HDACs, it is more likely that control is achieved by regulating the amount or the enzymatic activity of HAT and HDAC proteins through post-transcriptional or post-translational mechanisms.

Finally, the relative mRNA abundance in MII oocytes (either *in vivo*- or *in vitro*-matured) was not significantly different from the GV stage, showing that these transcripts do not undergo degradation during meiosis I in horse oocytes. Similar profiles for *HDAC1* and *HAT1* mRNAs have been previously observed in bovine oocytes (McGraw *et al.* 2003). On the other hand, two studies described a decrease in *HDAC1* mRNA during IVM in human oocytes (Wang *et al.* 2010; Huang *et al.* 2012). To the best of our knowledge, in these studies a mix of oligo-dT and random primers was used for reverse transcription, possibly introducing a bias for polyadenylated mRNA species rather than detecting a difference in the total mRNA abundance.

In the horse, IVM is applied to oocytes retrieved from antral follicles between 5 and 25 mm (10–25 mm in some laboratories). Larger follicles are not frequent and usually have a poor retrieval rate, therefore they cannot be consistently used. For this technical limitation we could not investigate whether IVM would equally affect GV oocytes collected from follicles ≥33 mm. In this vein, to the best of our knowledge, the diameter of the follicle of origin should be considered as one of the conditions inherent to IVM that, together with the other retrieval and culture procedures, might have contributed to the increased aneuploidy rate and altered epigenetic marks observed in our study.

To conclude, in the present study we characterised the phenotype and started to investigate the molecular events related

to IVM in an adult, naturally cycling, monovulatory species. This study also suggests that epigenetic instabilities triggered by IVM procedures may affect oocyte genetic stability.

Acknowledgements

The authors would like to thank Fabrice Vincent for support with laser scanning confocal microscopy (LSCM) and Guy Duchamp for collaborating with the collection of oocytes from the mares. This work was supported in part by 'Regione Sardegna and Regione Lombardia', project 'Ex Ovo Omnia' (Grant no. 26096200 to A. M. L.), by 'L'Oreal Italia per le Donne e la Scienza 2012' fellowship (Contract 2012 to F. F.), by FP7-PEOPLE-2011-CIG, Research Executive Agency (REA) 'Pro-Ovum' (Grant no. 303640 to V. L.) and by the Postdoctoral School of Agriculture and Veterinary Medicine, co-financed by the European Social Fund, Sectorial Operational Program for Human Resource Development 2007–2013 (Contract no. POSDRU/89/1.5/S/62371 to I. M.). The *in vivo* oocyte collection was financed by the Institut Français du Cheval et de l'Equitation.

References

Akiyama, T., Nagata, M., and Aoki, F. (2006). Inadequate histone deacetylation during oocyte meiosis causes aneuploidy and embryo death in mice. *Proc. Natl. Acad. Sci. USA* **103**, 7339–7344. doi:10.1073/PNAS.0510946103

Bartmann, A. K., Romao, G. S., Ramos Eda, S., and Ferriani, R. A. (2004). Why do older women have poor implantation rates? A possible role of the mitochondria. *J. Assist. Reprod. Genet.* **21**, 79–83. doi:10.1023/B:JARG.0000027018.02425.15

Campos-Chillon, F., Farmerie, T. A., Bouma, G. J., Clay, C. M., and Carnevale, E. M. (2015). Effects of aging on gene expression and mitochondrial DNA in the equine oocyte and follicle cells. *Reprod. Fertil. Dev.* doi:10.1071/RD14472

Carnevale, E. M. (2008). The mare model for follicular maturation and reproductive ageing in the woman. *Theriogenology* **69**, 23–30. doi:10.1016/J.THERIOGENOLOGY.2007.09.011

Chen, J., Melton, C., Suh, N., Oh, J. S., Horner, K., Xie, F., Sette, C., Blelloch, R., and Conti, M. (2011). Genome-wide analysis of translation reveals a critical role for deleted in azoospermia-like (*Dazl*) at the oocyte-to-zygote transition. *Genes Dev.* **25**, 755–766. doi:10.1101/GAD.2028911

Cheng, E. Y., Hunt, P. A., Naluai-Cecchini, T. A., Fligner, C. L., Fujimoto, V. Y., Pasternack, T. L., Schwartz, J. M., Steinauer, J. E., Woodruff, T. J., Cherry, S. M., Hansen, T. A., Vallente, R. U., Broman, K. W., and Hassold, T. J. (2009). Meiotic recombination in human oocytes. *PLoS Genet.* **5**, e1000661. doi:10.1371/JOURNAL.PGEN.1000661

Chiang, T., Duncan, F. E., Schindler, K., Schultz, R. M., and Lampson, M. A. (2010). Evidence that weakened centromere cohesion is a leading cause of age-related aneuploidy in oocytes. *Curr. Biol.* **20**, 1522–1528. doi:10.1016/J.CUB.2010.06.069

Choi, Y. H., Hochi, S., Braun, J., Sato, K., and Oguri, N. (1993). *In vitro* maturation of equine oocytes collected by follicle aspiration and by the slicing of ovaries. *Theriogenology* **40**, 959–966. doi:10.1016/0093-691X(93)90364-B

Clayton, A. L., Hazzalin, C. A., and Mahadevan, L. C. (2006). Enhanced histone acetylation and transcription: a dynamic perspective. *Mol. Cell* **23**, 289–296. doi:10.1016/J.MOLCEL.2006.06.017

Cox, L., Vanderwall, D. K., Parkinson, K. C., Sweat, A., and Isom, S. C. (2015). Expression profiles of select genes in cumulus–oocyte complexes from young and aged mares. *Reprod. Fertil. Dev.* doi:10.1071/RD14446

Donadeu, F. X., and Pedersen, H. G. (2008). Follicle development in mares. *Reprod. Domest. Anim.* **43**(Suppl 2), 224–231. doi:10.1111/J.1439-0531.2008.01166.X

Duncan, F. E., Chiang, T., Schultz, R. M., and Lampson, M. A. (2009). Evidence that a defective spindle assembly checkpoint is not the primary cause of maternal age-associated aneuploidy in mouse eggs. *Biol. Reprod.* **81**, 768–776. doi:10.1095/BIOLREPROD.109.077909

Eichenlaub-Ritter, U. (2012). Oocyte ageing and its cellular basis. *Int. J. Dev. Biol.* **56**, 841–852. doi:10.1387/IJDB.120141UE

Eichenlaub-Ritter, U., Vogt, E., Yin, H., and Gosden, R. (2004). Spindles, mitochondria and redox potential in ageing oocytes. *Reprod. Biomed. Online* **8**, 45–58. doi:10.1016/S1472-6483(10)60497-X

Emery, B. R., Wilcox, A. L., Aoki, V. W., Peterson, C. M., and Carrell, D. T. (2005). *In vitro* oocyte maturation and subsequent delayed fertilisation is associated with increased embryo aneuploidy. *Fertil. Steril.* **84**, 1027–1029. doi:10.1016/J.FERTNSTERT.2005.04.036

Franciosi, F., Lodde, V., Goudet, G., Duchamp, G., Deleuze, S., Douet, C., Tessaro, I., and Luciano, A. M. (2012). Changes in histone H4 acetylation during *in vivo* versus *in vitro* maturation of equine oocytes. *Mol. Hum. Reprod.* **18**, 243–252. doi:10.1093/MOLEHR/GAR077

Ginther, O. J. (2012). The mare: a 1000-pound guinea pig for study of the ovulatory follicular wave in women. *Theriogenology* **77**, 818–828. doi:10.1016/J.THERIOGENOLOGY.2011.09.025

Ginther, O. J., Gastal, E. L., Gastal, M. O., Bergfelt, D. R., Baerwald, A. R., and Pierson, R. A. (2004). Comparative study of the dynamics of follicular waves in mares and women. *Biol. Reprod.* **71**, 1195–1201. doi:10.1095/BIOLREPROD.104.031054

Goudet, G., Bezard, J., Duchamp, G., Gerard, N., and Palmer, E. (1997). Equine oocyte competence for nuclear and cytoplasmic *in vitro* maturation: effect of follicle size and hormonal environment. *Biol. Reprod.* **57**, 232–245. doi:10.1095/BIOLREPROD57.2.232

Hassold, T., and Hunt, P. (2001). To err (meiotically) is human: the genesis of human aneuploidy. *Nat. Rev. Genet.* **2**, 280–291. doi:10.1038/35066065

Hendriks, W. K., Colleoni, S., Galli, C., Paris, D. B., Colenbrander, B., Roelen, B. A., and Stout, T. A. (2015). Maternal age and *in vitro* culture affect mitochondrial number and function in equine oocytes and embryos. *Reprod. Fertil. Dev.* doi:10.1071/RD14450

Hinrichs, K., Schmidt, A. L., Friedman, P. P., Selgrath, J. P., and Martin, M. G. (1993). *In vitro* maturation of horse oocytes: characterisation of chromatin configuration using fluorescence microscopy. *Biol. Reprod.* **48**, 363–370. doi:10.1095/BIOLREPROD48.2.363

Homer, H. A., McDougall, A., Levasseur, M., Yallop, K., Murdoch, A. P., and Herbert, M. (2005). Mad2 prevents aneuploidy and premature proteolysis of cyclin B and securin during meiosis I in mouse oocytes. *Genes Dev.* **19**, 202–207. doi:10.1101/GAD.328105

Huang, J., Li, T., Ding, C. H., Brosens, J., Zhou, C. Q., Wang, H. H., and Xu, Y. W. (2012). Insufficient histone-3 lysine-9 deacetylation in human oocytes matured *in vitro* is associated with aberrant meiosis. *Fertil. Steril.* **97**, 178–184e3. doi:10.1016/J.FERTNSTERT.2011.10.023

Jones, K. T., and Lane, S. I. (2013). Molecular causes of aneuploidy in mammalian eggs. *Development* **140**, 3719–3730. doi:10.1242/DEV.090589

Klinker, H., Mueller-Planitz, F., Yang, R., Forne, I., Liu, C. F., Nordenskiold, L., and Becker, P. B. (2014). ISWI remodelling of physiological chromatin fibres acetylated at lysine 16 of histone H4. *PLoS One* **9**, e88411. doi:10.1371/JOURNAL.PONE.0088411

Li, X. C., Bolcun-Filas, E., and Schimenti, J. C. (2011). Genetic evidence that synaptonemal complex axial elements govern recombination pathway choice in mice. *Genetics* **189**, 71–82. doi:10.1534/GENETICS.111.130674

Lombardi, P. M., Cole, K. E., Dowling, D. P., and Christianson, D. W. (2011). Structure, mechanism and inhibition of histone deacetylases and related metalloenzymes. *Curr. Opin. Struct. Biol.* **21**, 735–743. doi:10.1016/J.SBI.2011.08.004

Luciano, A. M., Goudet, G., Perazzoli, F., Lahuec, C., and Gerard, N. (2006). Glutathione content and glutathione peroxidase expression in *in vivo*- and *in vitro*-matured equine oocytes. *Mol. Reprod. Dev.* **73**, 658–666. doi:10.1002/MRD.20469

Luo, Y. B., Ma, J. Y., Zhang, Q. H., Lin, F., Wang, Z. W., Huang, L., Schatten, H., and Sun, Q. Y. (2013). MBTD1 is associated with Pr-Set7 to stabilise H4K20me1 in mouse oocyte meiotic maturation. *Cell Cycle* **12**, 1142–1150. doi:10.4161/CC.24216

Luzzo, K. M., Wang, Q., Purcell, S. H., Chi, M., Jimenez, P. T., Grindler, N., Schedl, T., and Moley, K. H. (2012). High-fat diet-induced developmental defects in the mouse: oocyte meiotic aneuploidy and fetal growth retardation/brain defects. *PLoS One* **7**, e49217. doi:10.1371/JOURNAL.PONE.0049217

Ma, P., and Schultz, R. M. (2008). Histone deacetylase 1 (HDAC1) regulates histone acetylation, development and gene expression in preimplantation mouse embryos. *Dev. Biol.* **319**, 110–120. doi:10.1016/J.YDBIO.2008.04.011

Ma, P., and Schultz, R. M. (2013). Histone deacetylase 2 (HDAC2) regulates chromosome segregation and kinetochore function via H4K16 deacetylation during oocyte maturation in mouse. *PLoS Genet.* **9**, e1003377. doi:10.1371/JOURNAL.PGEN.1003377

Ma, J., Flemr, M., Strnad, H., Svoboda, P., and Schultz, R. M. (2013). Maternally recruited DCP1A and DCP2 contribute to messenger RNA degradation during oocyte maturation and genome activation in mouse. *Biol. Reprod.* **88**, 11. doi:10.1095/BIOLREPROD.112.105312

Marmorstein, R., and Zhou, M. M. (2014). Writers and readers of histone acetylation: structure, mechanism and inhibition. *Cold Spring Harb. Perspect. Biol.* **6**, a018762. doi:10.1101/CSHPERSPECT.A018762

McGraw, S., Robert, C., Massicotte, L., and Sirard, M. A. (2003). Quantification of histone acetyltransferase and histone deacetylase transcripts during early bovine embryo development. *Biol. Reprod.* **68**, 383–389. doi:10.1095/BIOLREPROD.102.005991

Nabti, I., Marangos, P., Bormann, J., Kudo, N. R., and Carroll, J. (2014). Dual-mode regulation of the APC/C by CDK1 and MAPK controls meiosis I progression and fidelity. *J. Cell Biol.* **204**, 891–900. doi:10.1083/JCB.201305049

Nichols, S. M., Gierbolini, L., Gonzalez-Martinez, J. A., and Bavister, B. D. (2010). Effects of *in vitro* maturation and age on oocyte quality in the rhesus macaque *Macaca mulatta*. *Fertil. Steril.* **93**, 1591–1600. doi:10.1016/J.FERTNSTERT.2008.12.141

Nogueira, D., Staessen, C., Van de Velde, H., and Van Steirteghem, A. (2000). Nuclear status and cytogenetics of embryos derived from *in vitro*-matured oocytes. *Fertil. Steril.* **74**, 295–298. doi:10.1016/S0015-0282(00)00642-7

Parthun, M. R. (2007). Hat1: the emerging cellular roles of a type B histone acetyltransferase. *Oncogene* **26**, 5319–5328. doi:10.1038/SJ.ONC.1210602

Peng, L., Ling, H., Yuan, Z., Fang, B., Bloom, G., Fukasawa, K., Koomen, J., Chen, J., Lane, W. S., and Seto, E. (2012). SIRT1 negatively regulates the activities, functions and protein levels of hMOF and TIP60. *Mol. Cell. Biol.* **32**, 2823–2836. doi:10.1128/MCB.00496-12

Rambags, B. P., Krijtenburg, P. J., Drie, H. F., Lazzari, G., Galli, C., Pearson, P. L., Colenbrander, B., and Stout, T. A. (2005). Numerical chromosomal abnormalities in equine embryos produced *in vivo* and *in vitro*. *Mol. Reprod. Dev.* **72**, 77–87. doi:10.1002/MRD.20302

Rambags, B. P., van Boxtel, D. C., Tharasanit, T., Lenstra, J. A., Colenbrander, B., and Stout, T. A. (2014). Advancing maternal age predisposes to mitochondrial damage and loss during maturation of equine oocytes *in vitro*. *Theriogenology* **81**, 959–965. doi:10.1016/J.THERIOGENOLOGY.2014.01.020

Requena, A., Bronet, F., Guillen, A., Agudo, D., Bou, C., and Garcia-Velasco, J. A. (2009). The impact of i*n vitro* maturation of oocytes on aneuploidy rate. *Reprod. Biomed. Online* **18**, 777–783. doi:10.1016/S1472-6483(10)60026-0

Roberts, R., Iatropoulou, A., Ciantar, D., Stark, J., Becker, D. L., Franks, S., and Hardy, K. (2005). Follicle-stimulating hormone affects metaphase I chromosome alignment and increases aneuploidy in mouse oocytes matured *in vitro*. *Biol. Reprod.* **72**, 107–118. doi:10.1095/BIOLREPROD.104.032003

Robin, P., Fritsch, L., Philipot, O., Svinarchuk, F., and Ait-Si-Ali, S. (2007). Post-translational modifications of histones H3 and H4 associated with the histone methyltransferases Suv39h1 and G9a. *Genome Biol.* **8**, R270. doi:10.1186/GB-2007-8-12-R270

Ruggeri, E., DeLuca, K. F., Galli, C., Lazzari, G., DeLuca, J. G., and Carnevale, E. M. (2015). Cytoskeletal alterations associated with donor age and culture interval for equine oocytes and potential zygotes that failed to cleave after intracytoplasmic sperm injection. *Reprod. Fertil. Dev.* doi:10.1071/RD14468

Sanfins, A., Lee, G. Y., Plancha, C. E., Overstrom, E. W., and Albertini, D. F. (2003). Distinctions in meiotic spindle structure and assembly during *in vitro* and *in vivo* maturation of mouse oocytes. *Biol. Reprod.* **69**, 2059–2067. doi:10.1095/BIOLREPROD.103.020537

Shin, Y. H., Choi, Y., Erdin, S. U., Yatsenko, S. A., Kloc, M., Yang, F., Wang, P. J., Meistrich, M. L., and Rajkovic, A. (2010). Hormad1 mutation disrupts synaptonemal complex formation, recombination and chromosome segregation in mammalian meiosis. *PLoS Genet.* **6**, e1001190. doi:10.1371/JOURNAL.PGEN.1001190

Shogren-Knaak, M., Ishii, H., Sun, J. M., Pazin, M. J., Davie, J. R., and Peterson, C. L. (2006). Histone H4–K16 acetylation controls chromatin structure and protein interactions. *Science* **311**, 844–847. doi:10.1126/SCIENCE.1124000

Shomper, M., Lappa, C., and FitzHarris, G. (2014). Kinetochore microtubule establishment is defective in oocytes from aged mice. *Cell Cycle* **13**, 1171–1179. doi:10.4161/CC.28046

te Velde, E. R., and Pearson, P. L. (2002). The variability of female reproductive ageing. *Hum. Reprod. Update* **8**, 141–154. doi:10.1093/HUMUPD/8.2.141

Tsutsumi, M., Fujiwara, R., Nishizawa, H., Ito, M., Kogo, H., Inagaki, H., Ohye, T., Kato, T., Fujii, T., and Kurahashi, H. (2014). Age-related decrease of meiotic cohesins in human oocytes. *PLoS One* **9**, e96710. doi:10.1371/JOURNAL.PONE.0096710

Turner, B. M. (2014). Nucleosome signalling: an evolving concept. *Biochim. Biophys. Acta* **1839**, 623–626. doi:10.1016/J.BBAGRM.2014.01.001

Wang, N., Le, F., Zhan, Q. T., Li, L., Dong, M. Y., Ding, G. L., Xu, C. M., Jiang, S. W., Huang, H. F., and Jin, F. (2010). Effects of *in vitro* maturation on histone acetylation in metaphase II oocytes and early cleavage embryos. *Obstet. Gynecol. Int.* **2010**, 989278. doi:10.1155/2010/989278

Yang, F., Baumann, C., Viveiros, M. M., and De La Fuente, R. (2012). Histone hyperacetylation during meiosis interferes with large-scale chromatin remodelling, axial chromatid condensation and sister chromatid separation in the mammalian oocyte. *Int. J. Dev. Biol.* **56**, 889–899. doi:10.1387/IJDB.120246RD

Yun, Y., Holt, J. E., Lane, S. I., McLaughlin, E. A., Merriman, J. A., and Jones, K. T. (2014). Reduced ability to recover from spindle disruption and loss of kinetochore spindle assembly checkpoint proteins in oocytes from aged mice. *Cell Cycle* **13**, 1938–1947. doi:10.4161/CC.28897

Zentner, G. E., and Henikoff, S. (2014). Regulation of nucleosome dynamics by histone modifications. *Nat. Struct. Mol. Biol.* **20**, 259–266. doi:10.1038/NSMB.2470